Diurnal variation in summer precipitation over the central Tibetan Plateau

Prasamsa Singh[1] and Kenji Nakamura[2]

Received 23 January 2009; revised 22 May 2009; accepted 15 July 2009; published 23 October 2009.

[1] The diurnal cycle of rainfall over the central Tibetan Plateau was investigated by examining data acquired by the Tropical Rainfall Measuring Mission Precipitation Radar during the summer monsoon season (June–August) from 1998–2007. High-spatial-resolution data ($\sim$5 km $\times$ 5 km) were used to identify the role of complex topographic features of the plateau. Diurnal variations in rain rate, frequency of rain, conditional rain rate, and storm-height were analyzed on a monthly basis to determine the characteristics of precipitation. The results are interpreted as precipitation characteristics in a semiarid region with weak prevailing winds. Distinct diurnal variation was seen over hilly regions, valleys, and lakes. Precipitation activity over the hilly region is generally strongest during the late afternoon. But in contrast, valleys and lakes show dominant late-evening peaks, and a secondary morning rainfall peak is distinctly evident over large lakes. However, the time of peak rain rate is delayed with increasing lake size. The shift in rain peak location toward lakes and valleys also appeared clearly.

Citation: Singh, P., and K. Nakamura (2009), Diurnal variation in summer precipitation over the central Tibetan Plateau, *J. Geophys. Res.*, *114*, D20107, doi:10.1029/2009JD011788.

1. Introduction

[2] Diurnal variation of rainfall is one of the most important characteristics over a region and is often related to physical processes governed by geographical features and atmospheric dynamics that control rainfall over that area. The pattern of diurnal variation of rainfall may change with season. Over the tropics, maximum rainfall over land and oceanic regions is observed during the late-afternoon and early-morning periods, respectively [*Hirose and Nakamura*, 2005; *Nesbitt and Zipser*, 2003; *Nitta and Sekine*, 1994; *Ohsawa et al.*, 2001]. The diurnal cycle of rainfall, usually dominated by the frequency of occurrence [*Dai et al.*, 2007], has large spatial and seasonal variations. Deep convection tends to organize on the mesoscale and undergoes an evolution characterized by a dominance of convective rainfall early in the life cycle followed by upscale growth and development of stratiform rainfall on a time scale of 2–4 h and longer [*Houze*, 1977; *Leary and Houze*, 1979; *Zipser*, 1977]. Drizzle and nonshowery rainfall occur frequently in the morning over most land areas, whereas convective activity occurs during late afternoon [*Dai*, 2001].

[3] *Lin et al.* [2000] suggested that the nocturnal maximum results from stratiform rain enhanced by instability due to nocturnal radiative cooling at the cloud top. *Kubota and Nitta* [2001] mentioned that water vapor accumulation at low levels in the evening contributes significantly to the development of nocturnal convection. *Nesbitt and Zipser* [2003] suggested that nocturnal rain in tropic is often caused by mesoscale convective systems (MCSs), rather than isolated convection and that MCSs are strongest after midnight, presumably owing to the upscale growth of afternoon convection. *Yu et al.* [2007] indicated that the early morning peak mainly comes from long-duration rainfall events that last longer than 6 h, whereas the late-afternoon peak mainly comes from rainfall events lasting less than 3 h.

[4] Throughout the Asian monsoon region, topography has a significant impact on local weather and rainfall [*Reihl*, 1954]. Late-night and early-morning rainfall is associated with terrain or terrain-induced local circulations [*Barros et al.*, 2000, 2004; *Bhatt and Nakamura*, 2005; *Singh et al.*, 2005; *Kuwagata et al.*, 2001; *Lang and Barros*, 2002; *Ueno et al.*, 2001]. However, an afternoon to early evening peak is rainfall in generally more common than a late-night to early-morning peak [*Barros and Lang.*, 2003; *Ohsawa et al.*, 2001; *Ueno et al.*, 2001]. *Barros et al.* [2000] suggested that daytime upslope/up-valley winds are more intense than their nocturnal downslope/down-valley counterparts, and nocturnal peaks are strongest at low elevations where blocking of flow is most active. *Kuwagata et al.* [2001] found that valleys with widths of about 160 km and depths of 100 m are the most effective topographic scales for water vapor accumulation. *Bhushan and Barros* [2007] showed that a localized hydraulic jump-like circulation drives strong return winds that converge over the central lowlands preceding the nighttime rainfall, lifting warm moist air at the mouth of the valley, thus initiating nocturnal convection. *Sato et al.* [2007] also suggested topography has large impacts on cloud formation over arid/semiarid regions.

[1]Graduate School of Environmental Studies, Nagoya University, Nagoya, Japan.
[2]Hydrospheric Atmospheric Research Center, Nagoya University, Nagoya, Japan.

0148-0227/09/2009JD011788

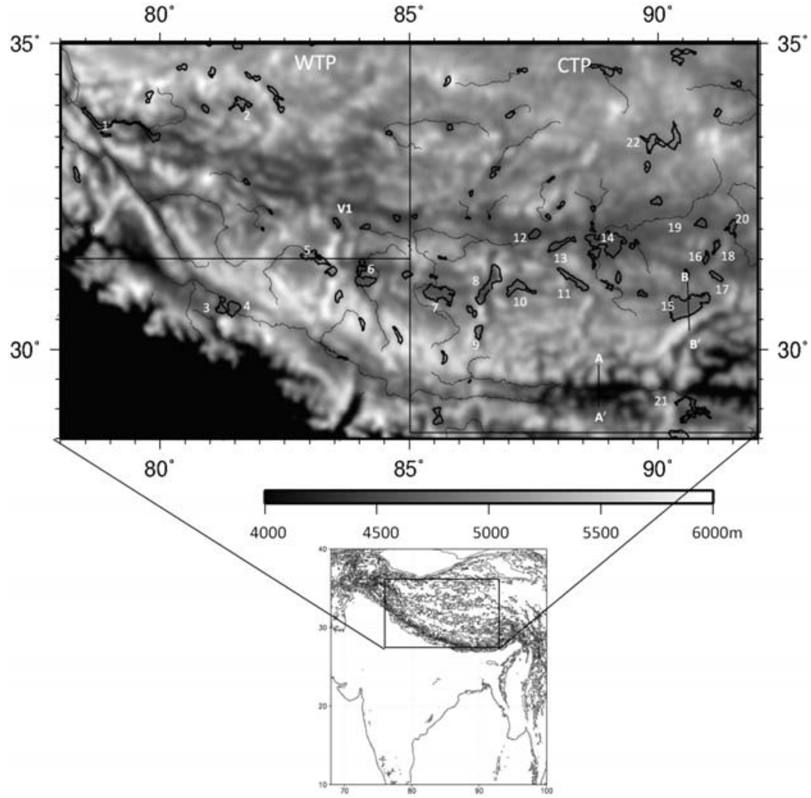

Figure 1. Map showing the region of study, including (top) terrain elevation (shaded, meters), rivers, and lakes and (bottom) the location of the study area. Lakes with numbers are as follows: 1, Banggong Co; 2, Lamajjangdand Co; 3, Langa Co; 4, Mapam Vam Co; 5, Ngamgla Ring Co; 6, Chabyr Caka; 7, Zhari Nam Co; 8, Tangra Yum Co; 9, Xuru Co; 10, Ngungze Co; 11, Gyaring Co; 12, Dagze Co; 13, Urru Co; 14, Siling Co; 15, Nam Co; 16, Bam Co; 17, Dogen Co; 18, Dung Co; 19, Zinge Tang Co; 20, Co Nag; 21, Yamzho Yum Co; and 22, Dorssodong Co. V1 refers to an east-west elongated valley at the center.

[5] It is well known that during summer, the Tibetan Plateau is a heat source to the atmosphere that generates significant diurnally varying circulations, vertical motions, and diabatic heating features on a large scale [*Flohn*, 1957; *Krishnamurti and Kishtawal*, 2000; *Li and Yanai*, 1996; *Luo and Yanai*, 1983; *Nitta*, 1983; *Yanai et al.*, 1992]. A study by *Fujinami and Yasunari* [2001] noted the contrast in diurnal cloud activity between spring and the summer monsoon season, with dry convection in spring and moist convection in summer associated with humidity. *Ueno et al.* [2001] revealed frequent rainfall with weak intensity over the Tibetan Plateau. Notable diurnal variations of convection over the plateau during the summer were also studied by *Murakami* [1987], *Yanai and Li* [1994], *Shimizu et al.* [2001], *Uyeda et al.* [2001], *Ohsawa et al.* [2001], and *Yamada and Uyeda* [2006]. *Wang et al.* [2004] documented a diurnal cycle of convection over the eastern Tibetan Plateau peaking in the late afternoon or early evening and then propagating eastward.

[6] The terrain of the Tibetan Plateau is complex, lying at an altitude of over 4000 m above mean sea level, and bejeweled with more than 1500 lakes, both large and small, which results in complex patterns of diurnal variation in precipitation. Figure 1 shows a topographic map of the Tibetan Plateau with numbers indicating the major 22 lakes used in this study. The plateau is situated north of the Himalayan range, on the leeward side with respect to the South Asian summer monsoon circulation, and thus receives less rainfall and very weak winds. *Yanai and Li* [1994] reported that the average wind speed is about 1.2 m s^{-1} in the early morning (0400–0600 local time (LT)) and has a maximum in the afternoon (1400–1800 LT) at about 5.0 m s^{-1} for May–August, based on data from the Global Atmospheric Research Program. As in other arid regions, the plateau receives rainfall maxima during the afternoon/early evening [*Banta*, 1998; *Tian et al.*, 2005]. A similar feature appeared in the current study, using data from the Tropical Rainfall Measuring Mission (TRMM) Precipitation Radar (PR) for 1998–2007, during June–August (Figure 2). More than 60% of daily rainfall appeared in the afternoon over the Tibetan Plateau, the Deccan Plateau and the Thar Desert when normalized morning (0000–1200 LT) rain rate subtracted from afternoon (1200–2400 LT) (Figure 2). Dark areas in Figure 2 are afternoon rain-enhanced regions.

[7] We hypothesized that local-scale phenomena (lake-land contrast and ridge-valley effects) would have their greatest impact on rainfall distributions where large-scale dynamical processes are weak. Some studies have been performed over the Tibetan Plateau to explain the role of topography on convective systems [*Fujinami et al.*, 2005] and some mechanisms have been proposed on the basis of numerical experiments [*Kuwagata et al.*, 2001]. However, a

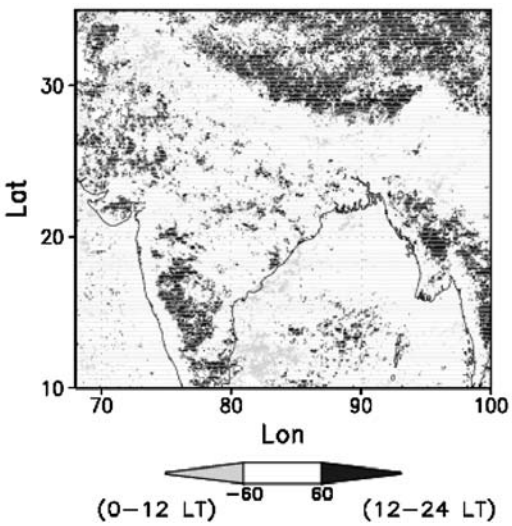

Figure 2. Rain fraction (%) difference between morning (0000–1200 LT) and afternoon (1200–2400 LT) for June, July, and August. Light shading shows morning-dominant regions, and dark shading shows afternoon-dominant regions.

detailed study has not been done with a long-term data set. This is because, in general, it is difficult to maintain routine observational stations in the desert and mountainous regions [*Ueno et al.*, 2007]. Most studies have been done with large spatial-scale data sets and using cloud data. However, cloud distributions are not always identical to rainfall distributions (see the study of *Tian et al.* [2005], based on GOES IR data). In order to determine the effects of topography over complex terrain, fine-scale data covering the diurnal cycle are essential. Satellite remote sensing with high-resolution footprints is the best tool to evaluate meteorological elements over such a heterogeneous area. The TRMM satellite can sample the diurnal cycle because of its non-Sun-synchronous orbit. The TRMM PR uniquely and directly observes rainfall from space at fine resolution ($\gtrsim$5 km) and has provided a rainfall data set for more than 10 years from 1998 until the present. Over land, the TRMM Microwave Imager, which is useful for rain mapping over oceans, has poor accuracy. However, the PR does not suffer from this limitation. Figure 2 demonstrates the necessity for the TRMM PR's diurnal sampling.

[8] The purpose of the study was to investigate diurnal variations in rainfall and to understand the effect of the surface topography, including lakes, over the central Tibetan Plateau. We used a TRMM PR data set with a grid size of $0.05^\circ \times 0.05^\circ$ latitude/longitude, focusing on the monthly progression of the summer monsoon season (June–August).

[9] The paper is organized as follows: section 2 describes the data sets and analysis method; results are presented in section 3; a discussion is presented in section 4; and section 5 includes the summary and conclusions.

2. Data and Methodology

[10] For the study of diurnal variation of rainfall, TRMM PR 2A25 [*Iguchi et al.*, 2000] instantaneous data for 1998–2007 were used. The Global 30 Arc Second Elevation (GTOPO30) data set was used for topography (http://edcdaac.usgs.gov/gtopo30/gtopo30.html).

[11] The National Aeronautics and Space Administration (NASA) and the Japan Aerospace Exploration Agency (JAXA) provided TRMM data products. We used level 2 Precipitation Radar data, Version 6, for the period 1998–2007. Product 2A25 provided the near-surface rain rate from the PR. Algorithms for rain rate and rain types were described by *Iguchi et al.* [2000] and *Awaka* [1998], respectively. "Near surface" was defined as the lowest point in the clutter-free ranges in almost all cases. The near-surface height ranged from 500 m above ground level (AGL) at nadir to 2 km AGL at the swath edge.

[12] Rain rate was calculated as a product of the conditional rain rate (near-surface rain rate >0 mm h^{-1}) and the frequency of rain (number of rain samples normalized by total number of samples). Amount of rainfall (rainfall) is accumulation of rain for a certain period. The PR 2A23 data [*Awaka*, 1998] provided "storm height." Storm height is the height of the storm top (>18 dBZ: a reflectivity equivalent to about 0.5 mm h^{-1}). In this article, storm-height data were picked up only when rain existed at the near-surface height in 2A25.

[13] *Fu and Liu* [2007] suggested that the TRMM PR algorithm version 5 and 6 misidentifies weak convective rain events as stratiform rain events over the plateau. They suggested that this may be due to the fact that the freezing level is close to the surface. *Schumacher and Houze* [2003] also suggested that the PR algorithm from version 5 of TRMM identified shallow, isolated cells as stratiform. Regarding this problem, we did not use the rain type provided in the 2A23 data set in this study.

[14] In order to obtain climatological characteristics, gridded data were generated from the instantaneous data on a grid size of 0.05° longitude by 0.05° latitude for 24 1-h intervals. This grid size is almost equal to the PR pixel size.

[15] Figure 3a shows the rain rate (mm/d) distribution over the Tibetan plateau for June–August of 1998–2007 (details of Figure 3 will be discussed in section 3). Figure 3a depicts the distribution of rain varying strongly from east to west, and the absolute rain rate may not properly show characteristics of the diurnal variation. So, we have expressed the rain rate distribution in terms of rain fraction (RF) as

$$RF_h = \frac{R_h}{\sum\limits_{h=1}^{24} R_h},$$

where R is rain rate and. h is local time in hours.

[16] In this study, the 24-h period is divided into 8 periods of 3 h duration as follows: late night (0000–0300 LT), early morning (0300–0600 LT), morning (0600–0900 LT), late morning (0900–1200 LT), early afternoon (1200–1500 LT), late afternoon (1500–1800 LT), evening (1800–2100 LT), and night (2100–2400 LT). Here, the local time is time displacement from UTC, calculated from longitude. *Hirose et al.* [2008] found that the diurnal signature over the Tibetan Plateau showed a high degree of spatial uniformity.

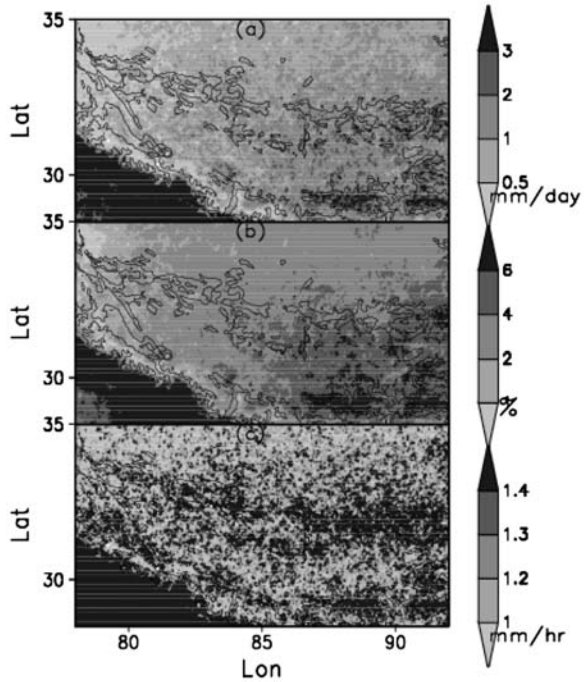

Figure 3. Average during June, July, and August (JJA) for (a) amount of rainfall (mm/d), (b) frequency of rain (%), and (c) conditional rain rate (mm/h). White line indicates the 4700-m elevation contour.

However, they found the signature of diurnal variation was still noisy owing to fluctuations resulting from sampling effects.

[17] In the present study, hourly rain rate totals were smoothed by using a 1:2:1 smoothing filter. Smoothed rain rate (SR) is given as

$$SR_h = \frac{R_{h-1} + 2R_h + R_{h+1}}{4},$$

where R and h denote the rain rate and local time in hours, respectively, as in the case of rain fraction computation.

[18] We used the coefficient of variation (CV) to compare parameters that have different means. The CV is a normalized measure of dispersion of a distribution defined as the ratio of the standard deviation (σ) to the mean (μ),

$$CV = \frac{\sigma}{\mu}.$$

The strength of the diurnal variation was also analyzed by the coefficient of variation over 24 h.

[19] For the study of surface height, we used the Global 30 Arc Second Elevation data Set (GTOPO30), produced by the Earth Resources Observation Systems (EROS) Data Center of the U. S. Geological Survey. The original data of 30 s spatial resolution were interpolated onto a $0.05° \times 0.05°$ grid.

[20] Because the plateau has complex topography, we applied a band-pass filter for subtracting wide-scale filtered data ($0.35° \times 0.35°$) from the fine-scale filtered data ($0.05° \times 0.05°$) to reveal the relationship between spatially small undulations in surface height and rain rate. Then, the R-squared (square of correlation coefficient) statistic was used to determine the relationship between rain rate and surface roughness. As a measure of surface roughness, the standard deviation of surface height was calculated at each $0.05° \times 0.05°$ grid point from the surrounding $0.75° \times 0.75°$ domain.

[21] The issue of sampling error requires careful attention. The PR swath is less than 250 km in width, and the statistical significance of rain events over semiarid regions may be poor. However, by using 10 years of JJA data, the result should be reliable. As our study area was situated on the margin of the tropical zone, the number of TRMM overpasses was at its highest. The orbital pattern of the satellite allows sampling ranging from 0.8 times per day at 28.5°N to nearly twice per day at 35°N over a 0.05×0.05 grid box. On an average, the number of samples is 1 per day at 31°N. Assuming a frequency of rain about 5%, approximate 0.6 rain overpasses occur in the region in a single 1-h interval for 30 months (3 months $\times$ 10 years). This problem is mitigated by spatial averaging. In this case, we averaged across the central Tibetan Plateau (CTP) (85°E–92°E, 28.5°N–35°N, shown in Figure 1), which has a size of $7° \times 6.5°$ latitude/longitude. Assuming a typical independent size for precipitation statistics of $0.5° \times 0.5°$, the number of rain cells for one month for one local hour becomes about 110, which may be sufficient. If we assume that the rain occurrence obeys a binomial distribution with occurrence probability (p), the average number of occurrences and its variance are np and $np\ (1 - p)$, respectively, where n is the number of samples. In our case, np is 110, and the standard deviation becomes about 10 corresponding to about 9% of the number of events. We smoothed the diurnal variation by 1:2:1 weighting, which further reduces the standard deviation to about 6%. In fact, in a separate analysis, we compared results for the first 5 years (1998–2002) and the last 5 years (2003–2007) and confirmed the consistency of findings.

[22] Later we will show the diurnal variation of precipitation over lakes. Table 1 shows the sizes and number of samples and rain pixels over lakes for 30 months (3 months $\times$ 10 years) depending on size and location of lakes. Lake

Table 1. Statistics of Lake Sizes, Approximate Sample Size, and Number of Rain Pixels for 3 Months for 10 Years for Lakes Used in This Study

Lake Number	Approximate Area (km^2)	Approximate Number of Samples, 3 months $\times$ 10 years	Approximate Number of Rain Pixels, 3 months $\times$ 10 years
15	1750	58,450	2800
14	1600	60,480	2560
7	900	30,600	1440
8	450	15,480	900
6	425	14,620	510
11	375	12,750	750
10	350	11,900	700
19	175	6580	490
12	150	5880	240
9	150	4890	240
16	125	4650	300
20	100	3920	280
17	75	2550	150
18	75	2820	180

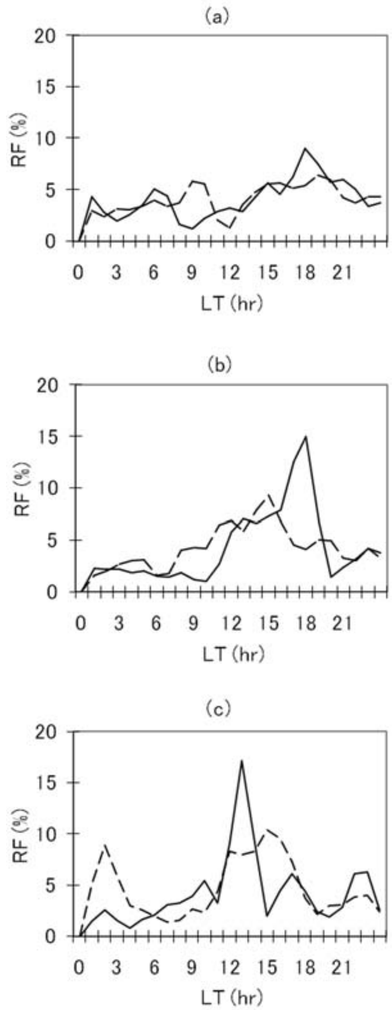

Figure 4. Diurnal variation in rain fraction (%) for 1998–2002 (solid line) and 2003–2007 (dashed line) for lakes (a) 15, (b) 19, and (c) 17.

sizes vary from 75 km^2 to 1750 km^2 and the number of rainy pixels varies approximately from 180 to 2800 for 30 months. Thus, the sampling issue varies highly with lake size.

[23] Figure 4 shows diurnal variation of rain fraction for the first 5 years (1998–2002, with solid line) and last 5 years (2003–2007, dashed line) for lakes of various sizes (lakes 15, 17 and 19). Even though the variations in the two periods are not identical, the result shows characteristics of lakes. For example, clear morning and evening peaks over lake 15, an afternoon peak over lakes 19 and 17.

3. Results

3.1. Seasonal and Intraseasonal Pattern of Diurnal Variation

[24] Results indicated that precipitation over the plateau is highest, at about 3.5 mm/d for JJA, over the southeastern part (Yarlung Zanbo river valley) and gradually decreases toward the northwestern part of the study area, which receives less than 0.5 mm/d (Figure 3a). The distribution of precipitation corresponds to the annual isohyetal map observed by *Yin et al.* [2008] using 94 weather stations over the Plateau. The frequency of rain occurrence also shows a pattern similar to the rain rate, varying from about 7% in the central part of the Tibetan Plateau to about 1% over the western part (Figure 3b). Conditional rain rate is, however, higher over local topographic minima (less than 4700 m), varying from about 0.5 mm/h to 1.6 mm/h over the region (Figure 3c). *Ueno et al.* [2001] also revealed frequent rainfall with weak intensity over the plateau.

[25] Because the precipitation distribution varies from east to west, in this study the Tibetan Plateau is separated into two parts: CTP and the western Tibetan Plateau (WTP) (78°E–85°E, 31.5°N–35°N, shown in Figure 1). The spatial coefficient of variation of rain rate over the CTP for June, July, and August (JJA) is 0.1, whereas it is 0.2 over the WTP. The large variation over the WTP may be due to the small number of rain samples that resulted from the low frequency of rain. Thus, hereafter, the study focuses on rain over the CTP.

[26] The diurnal cycle of rain rate during JJA over the CTP is much higher than during March, April, and May (MAM) and September, October, and November (SON) (Figure 5). Figure 5 shows local time versus rain rate (mm/h) averaged over CTP. December, January, and February (DJF) were not included because the TRMM PR observed very little precipitation. All seasons have peaks in the late afternoon period (around 1600 LT). Figure 5 also reveals that the summer season (JJA) receives the highest rain rate (0.13 mm/h) followed by SON. JJA receives more than 70% of the annual amount of rainfall. *Fujinami and Yasunari* [2001] suggested that summer seasons have distinct diurnal cloud activity over the Tibetan Plateau, with high humidity and temperature in the lower troposphere, which corresponds to strong diurnal variations of precipitation during JJA. However, the result is different from the diurnal variation over the southern part of the Himalayas, where the diurnal variation is strongest for MAM [i.e., *Bhatt and Nakamura*, 2006]. As JJA receives the highest amount of rainfall and has the highest diurnal variation in rain rate, we studied the summer period in further detail.

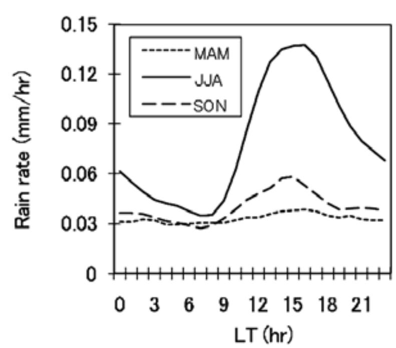

Figure 5. Diurnal time series of rain rate(mm/h) for March, April, and May (MAM), June, July, and August (JJA), and September, October, and November (SON) over the CTP.

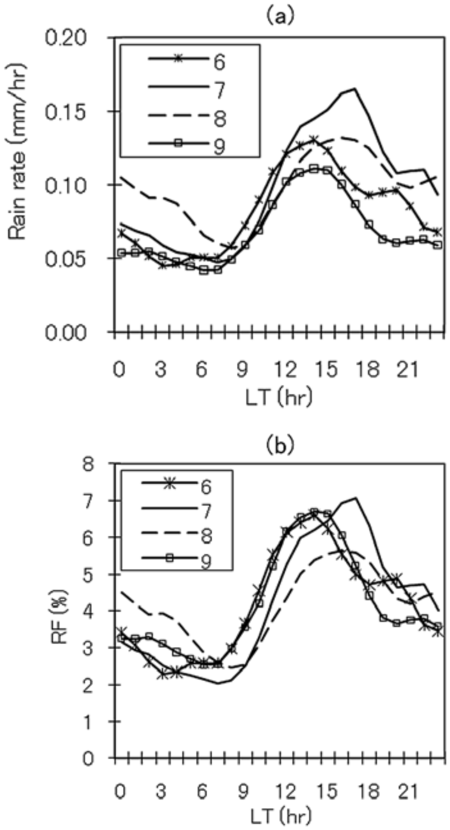

Figure 6. Diurnal time series during June (line 6), July (line 7), August (line 8), and September (line 9) over the CTP for (a) rain rate (mm/h) and (b) rain fraction (%).

[27] Diurnal variation in rain from June to September (JJAS) over the region was studied separately here on a monthly basis over the CTP, to see the seasonal progression. Although the study concentrated on JJA, September was included to illustrate the seasonal trend (Figure 6). Figure 6a shows that July receives the highest averaged rain rate (0.1 mm/h), and September receives the lowest averaged rain rate (0.07 mm/h). In order to compare diurnal variations for each month, we calculated the rain fraction for each month (Figure 6b). June and September have afternoon peaks around 1500 LT, whereas July and August have evening peaks around 1800 LT. July and August reveal the highest and least diurnal variation in rain rate, respectively (Figure 6b). Rain rate shows a distinct morning peak around 0300 LT in August (Figure 6).

[28] Each month exhibited individual characteristics. Figure 7 shows diurnal variation in frequency of rain and conditional rain rate, expressed as a percentage of the 24 h total. During June the peak of conditional rain rate occurs around 1400 LT but frequency of rain fluctuates highly. Peaks of conditional rain rate and frequency of rain during September occur almost at the same time, around 1500 LT. If we interpret high frequency of rain as persistent rain or stratiform wide spread rain, then July and August have convective (high conditional rain rate) rainfall during the afternoon around 1500 LT, followed by persistent (high frequency) rainfall. August shows more persistent rainfall during the morning around 0300 LT than does any other month (Figure 7). *Zipser* [1977], *Houze* [1977], and *Leary and Houze* [1979] also found deep convection, characterized by a dominance of convective rainfall early in the life cycle, followed by development of stratiform rainfall on a time scale of 2–4 h and longer. *Kondo et al.* [2006] showed that convective rain is followed by widespread rain over the tropical western Pacific using TRMM microwave radiom-

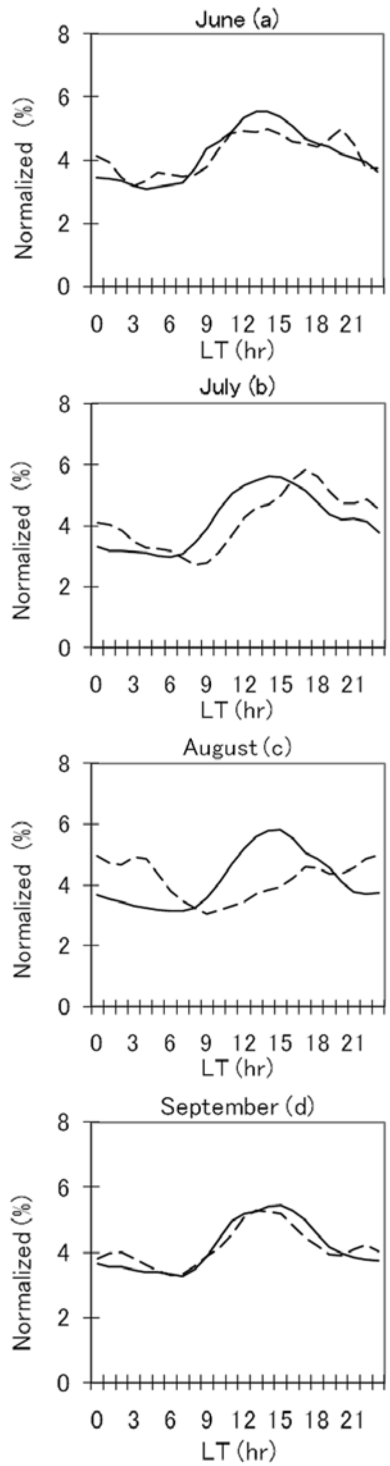

Figure 7. Diurnal time series of frequency of rain (dashed line) and conditional rain rate (solid line) fraction (%) for (a) June, (b) July, (c) August, and (d) September.

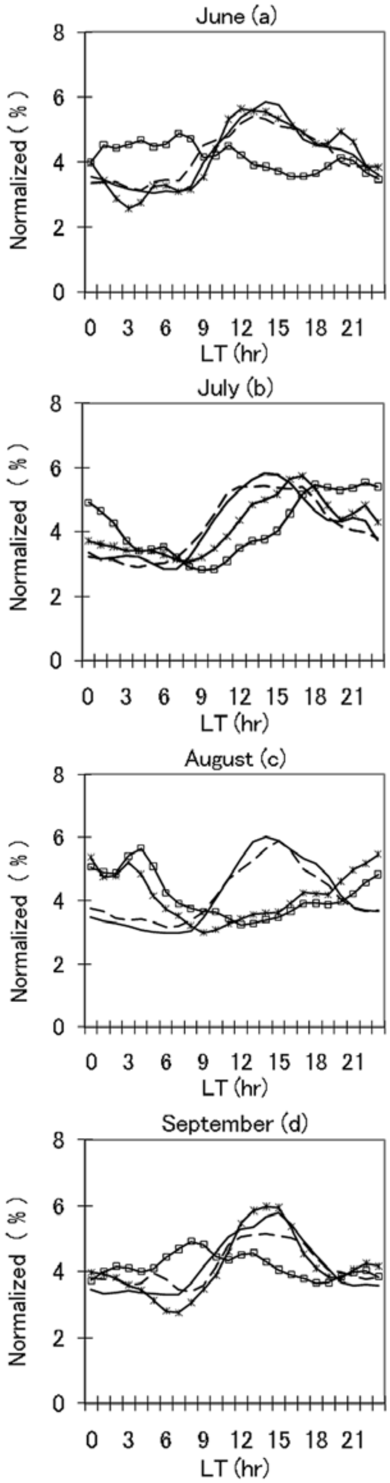

Figure 8. Diurnal time series of normalized conditional rain rate expressed as a percentage for 1998–2002 (solid line) and 2003–2007 (dashed line) and frequency of rain expressed as a percentage for 1998–2002 (solid line with crosses) and 2003–2007 (solid line with squares) over the CTP for (a) June, (b) July, (c) August, and (d) September.

eter and PR data. *Yamamoto et al.* [2008] also described a similar situation, but with regional differences, using TRMM data. They suggested that the regions showing a systematic difference between peak times for conditional rain rate and frequency of rain correspond to a high frequency of convective type rain. *Yamada and Uyeda* [2006] also observed late-night rainfall in August, which occurred in nonconvective systems. This resembles the results of our study.

[29] In order to check the consistency, we have compared the first 5 years (1998–2002) and second 5 years (2003–2007) over the region for June, July, August and September for frequency of rain and conditional rain rate (Figure 8). During June and September the peak of conditional rain rate is consistent; however, frequency of rain fluctuates. For July and August, although the trends for the two different periods are not same, the peak of conditional rain rate and frequency of rain are similar for the two periods.

[30] Figure 9 shows diurnal variation in storm height from June to September (JJAS). Diurnal variation in storm height is strong during July and August. July has a storm height peak earlier and broader than August as the peak of conditional rain rate.

3.2. Spatial Difference of Diurnal Variation During Summer

[31] The 3-hourly distribution of rain rate expressed as rain fraction (%) is shown in Figure 10. The central Tibetan plateau has late-afternoon-dominant rainfall. During the early-morning (0300–0600 LT) and late-morning periods (0600–0900 LT) about 15% of rainfall appeared to be mostly over lakes (lake numbers 1–22 except 3, 6, 10, 11, 16, and 20). *Bhatt and Nakamura* [2005] and *Negri et al.* [1994] also found morning rainfall over rivers. On the other hand, during the morning (0600–0900 LT) period, minimum rainfall occurs over other regions. During late morning (0900–1200 LT), rainfall appears over hilly regions, whereas rainfall diminishes over many lakes (1–12) and valleys (Yarlung Zanbo river valley). During early afternoon (1200–1500 LT), rainfall over the hilly regions is enhanced; on the other hand, rainfall decreases significantly over lakes (1–21 except 12, 15, 17–20) and deep valleys (Yarlung Zanbo river valley). Overall, the plateau receives its highest amount of rainfall during late afternoon (1500–1800 LT). Many researchers [*Hirose and Nakamura*, 2005; *Nitta and Sekine*, 1994; *Nesbitt and Zipser*, 2003; *Ohsawa et al.*, 2001] also found similar characteristics in many areas over land.

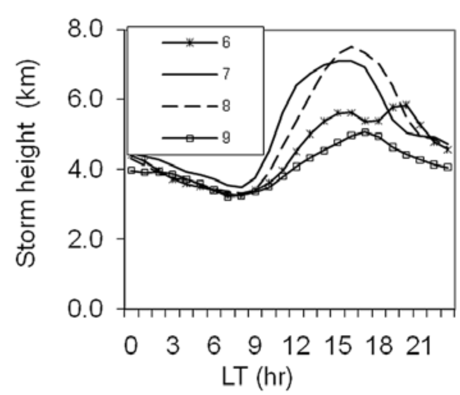

Figure 9. Diurnal time series of storm height (kilometers) for June (line 6), July (line 7), August (line 8), and September (line 9) over the CTP.

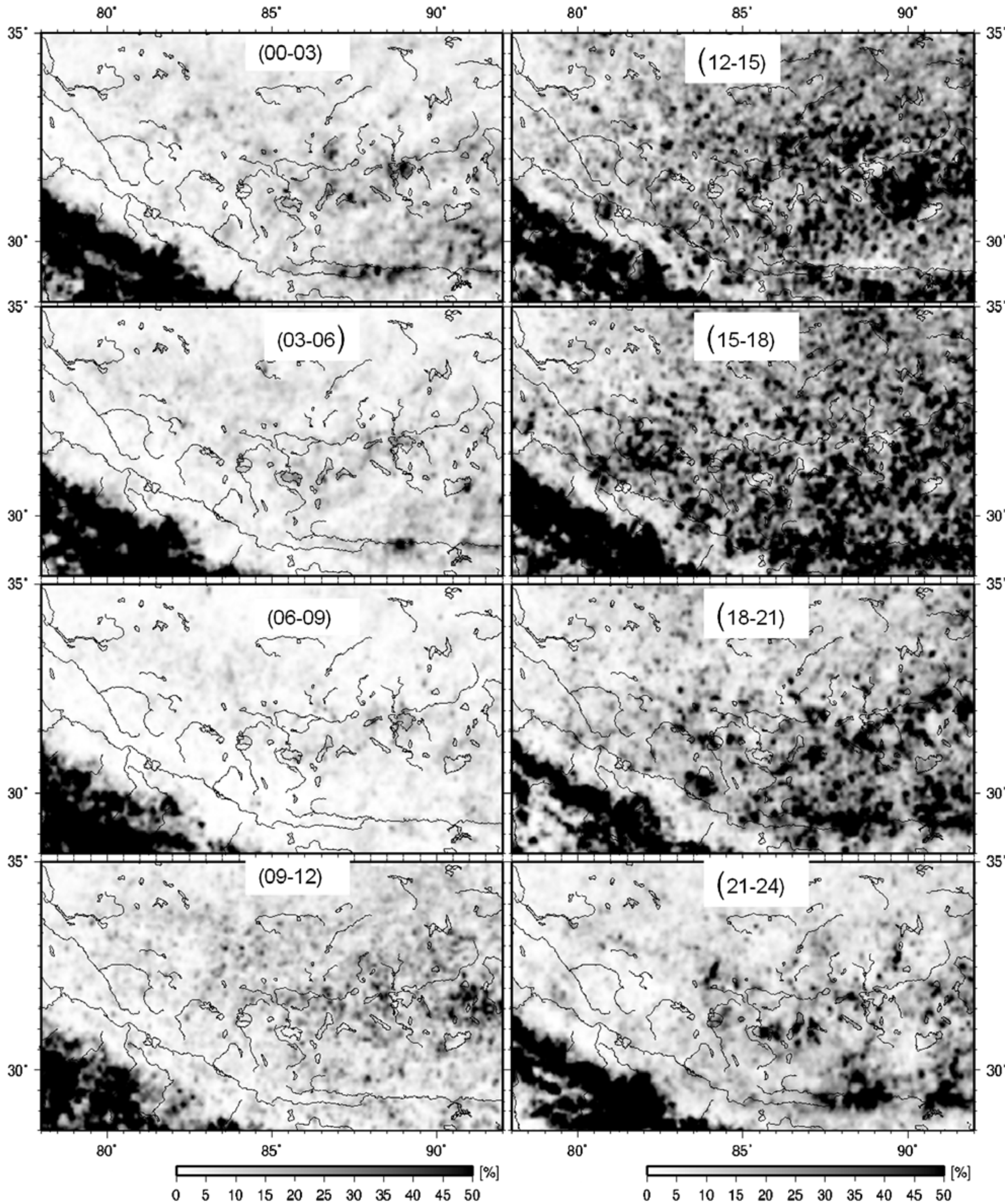

Figure 10. Mean 3-hourly rain fraction (%) distributions for JJA. Rivers and lakes are shown.

[32] During 1800–2100 LT, the rainfall diminishes almost all over the region of the Tibetan Plateau and concentrates over low lands (Yarlung Zanbo river valley, eastern part of V1) and lakes (1–20). During 2100–2400 LT rainfall is concentrated distinctly over deep valleys (Yarlung Zanbo river valley) and lakes (1–19 except 5 and 14). *Fujinami et al.* [2005] also found that cloud cover frequency (CCF) for high cloud and precipitation increased after 1300 LT over mountain ranges along 28.5°N and 30.2°N, reaching a maximum near 1800 LT and moved toward the valley area along 29.3°N.

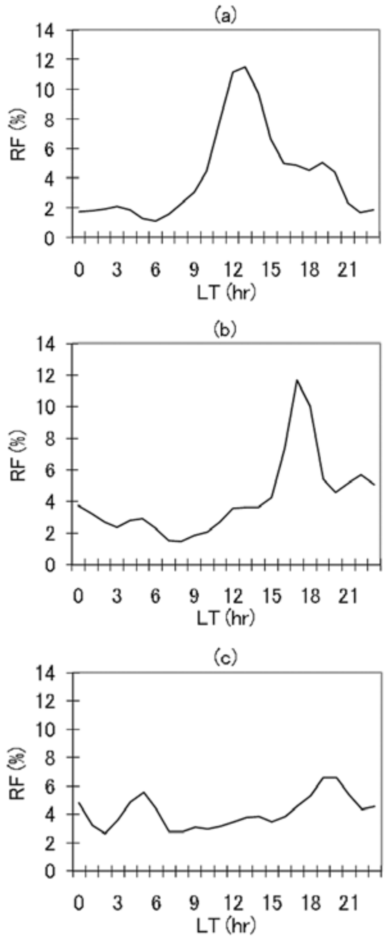

Figure 11. Diurnal time series of rain fraction (%) during JJA over (a) hilly region, (b) Yarlung Zanbo river valley, and (c) lake 15.

[33] It is also apparent that most lakes have peaks after evening. However, some lakes (e.g., 16, 17, and 19) have rainfall peaks during the afternoon, as is seen over hilly regions.

3.3. Diurnal Cycle of Rainfall Induced by Land-Lake Effect and Upslope/Downslope Flow

[34] In this section, we show the diurnal variations of rainfall over valleys and lakes in detail. Figure 11 shows diurnal variation in rain fraction over the hilly region, a valley and a lake. It should be noted that hilly regions (e.g., averaged over 33.5°N–34.5°N, 91°E–92°E) have a major afternoon peak around 1200 LT. Valleys (e.g., the basin of Yarlung Zanbo river valley, 29.2°N–29.3°N, 88.5°E–89.5°E) have major evening peaks around 1800 LT, and Lake 15 (shown in Figure 1) clearly has a major evening peak around 1900 LT with a distinct minor peak during the morning period around 0600 LT (Figure 11). It is also noted that the amplitude of diurnal variation over the lake is lower than the valley and the hilly region.

[35] Figure 12a shows afternoon (1200–1800 LT) rainfall minus evening rainfall (1800–2400 LT) over the CTP. Because afternoon rainfall occurs mostly over highland regions (hilly region) and evening rainfall occurs generally over lowland regions (valleys and lakes), two subregions were prepared as follows. Type I: afternoon (1200–1800 LT) rainfall is higher than evening rainfall (1800–2400 LT), and Type II: evening rainfall is higher than afternoon rainfall. Subregion Types II and I are averaged over the CTP region to analyze their diurnal variation.

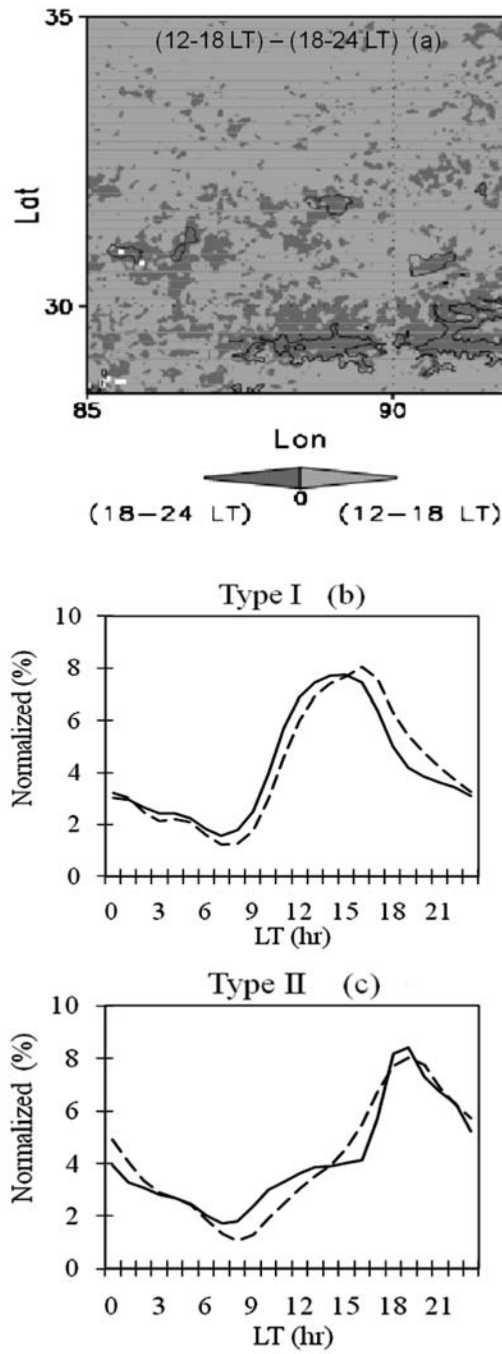

Figure 12. (a) Rain fraction difference between evening (1800–2400 LT) and afternoon (1200–1800 LT) in JJA. Light shading shows Type I regions, and dark shading shows Type II regions. Diurnal time series over (b) Type I regions and (c) Type II regions for normalized conditional rain rate (solid line) and frequency of rain expressed as a percentage (dashed line). Contour line is for elevation 4700 m.

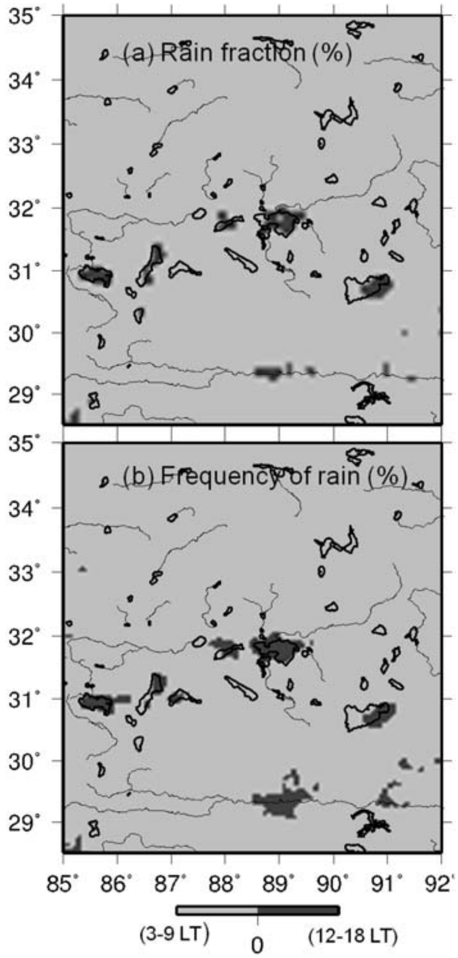

Figure 13. Fraction difference between morning (0300–0900 LT) and afternoon (1200–1800 LT) in JJA for (a) rain rate (%) and (b) frequency of rain (%). Dark shading shows morning-dominant regions, and light shading shows afternoon-dominant regions.

[36] Type I reveals a broad major peak during the afternoon (Figure 12b). Type II shows a narrow peak for both frequency of rain and conditional rain rate during the evening (Figure 12c). Type II exhibits diurnal variation with contemporaneous convective (high conditional rain rate) and persistent rainfall (high frequency of rain), whereas Type I shows convective rain maxima followed by persistent rainfall. Type I has stronger diurnal variation than Type II.

[37] It was also observed that the strength of diurnal variation of rainfall is less for the morning-dominant regions (morning rainfall (0300–0900 LT) > afternoon rainfall (1200–1800 LT) than afternoon-dominant regions and evening-dominant regions (figure not shown).

[38] In section 3.2, distinct morning (0300–0600 LT) rainfall appeared over most of the lakes and decreased during early afternoon (1200–1500 LT). Figure 13 shows rain rate and frequency of rain during the afternoon period (1200–1800 LT) minus the morning period (0300–0900 LT) over the CTP. Figure 13a shows that many lakes (7–9, and 13–15) and the Yarlung Zanbo river valley receive morning rainfall in contrast to afternoon rainfall. Figure 13b shows that the higher frequency of rain during morning rainfall over lakes (7, 8, 10 and 13–15) and the Yarlung Zanbo river valley than in afternoon period.

[39] The diurnal variations over valleys and lakes may vary depending upon topography, area, and depth of the basin. From earlier results, we found that some ridges are dominated by afternoon rainfall, whereas valleys are characterized by evening and late-night rainfall. *Kuwagata et al.* [2001] suggested precipitable water decreases during daytime in valley areas, while it increases over mountain ranges, using valleys with widths of about 160 km and depths of 100 m over the central Tibetan Plateau. We made a general assumption that valleys with a high surface roughness and a wide basin would have strong morning and evening rainfall. If analyses are based on the absolute altitude, the basin effect may be obscured because the same sized basin at high altitude and low altitude may have the same diurnal characteristics. To remove dependence on absolute altitude, we applied a spatial band-pass filter to surface elevation data. Surface roughness was measured by the local standard deviation of elevation. Figure 14a shows the correlation between local deviation of the band-pass-filtered elevation and diurnal variation of rain fraction ((1200–1800 LT) – (0300–0900 LT)). Figure 14a shows a positive correlation after application of the filter, although the correlation factor (R^2) is as small as 2%. This suggests that morning rainfall (0300–0900 LT) occurs over relatively low land and afternoon rainfall (1200–1800 LT) occurs over relatively high land. When we selected grid points with high surface roughness only (standard deviation >400 m), the correlation factor increased to 6% (Figure 14b). Although

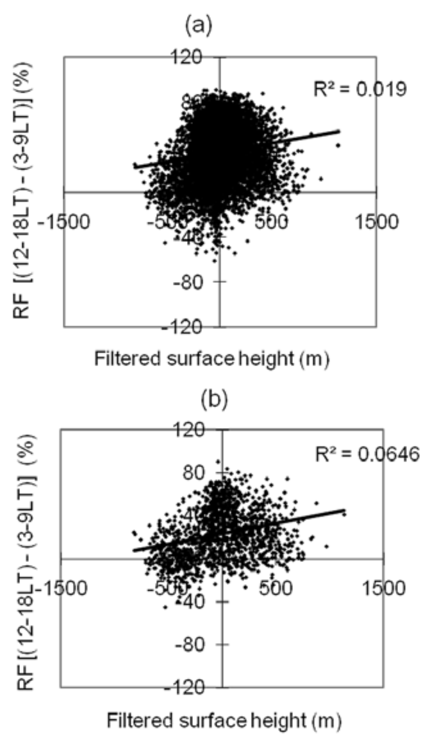

Figure 14. Scatter diagram of band-pass-filtered topography (meters) versus rain fraction expressed as a percentage difference ((1200–1800 LT) – (0300–0900 LT)) over (a) the whole CTP region and (b) only the highly variable region (standard deviation >400 m) over the CTP region.

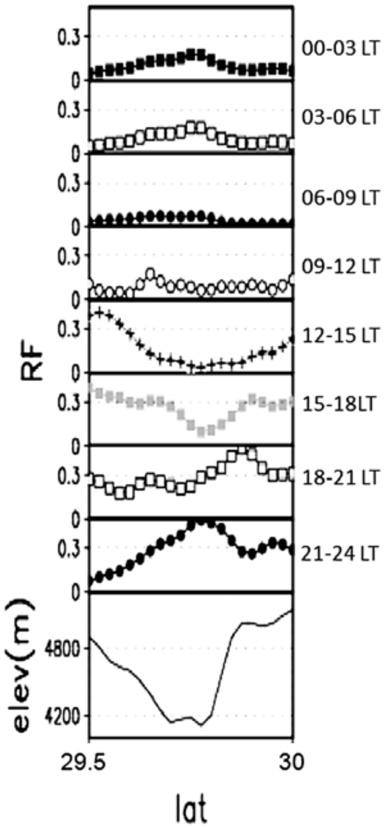

Figure 15. First through eighth panels show rain fraction distribution across Yarlung Zanbo river valley (line AA′ in Figure 1). Ninth panel shows basin elevation (meters) of the valley.

the correlation factor is low, the data show a reasonable trend. For a similar study of the correlation between diurnal variation ((1200–1800 LT) – (1800–2400 LT)) with and without selection of surface roughness, the correlation factor was calculated as 4% and 1%, respectively (figures not shown). Our results appear to agree with the results by *Kuwagata et al.* [2001], although we did not investigate the correlations using various band-pass filters.

[40] A shift in rain peak over the deep valleys (Yarlung Zanbo river valley) is apparent. Figure 15 shows the shift in rain peak over the Yarlung Zanbo river valley (AA′ in Figure 1). During 1200–1500 LT the rainfall is at a minimum over the valley. During 1500–1800 LT the rainfall peak shifts toward the valley from ridges and converges during 2100–2400 LT in the valley. During 0000–0300 LT the rainfall diminishes over the valley. Then during 0900–1200 LT the rainfall peak shifts toward ridges from the valley. *Fujinami et al.* [2005] also found similar characteristics, suggesting formation and development of convective type clouds and phase differences in the diurnal cycle were strongly affected by topography.

[41] In section 3.2 we showed that diurnal variations over the various lakes are different. This difference may depend on the sizes of the lakes and the steepness of the topography surrounding the lakes. We studied 14 lakes in detail (described in Table 1). From section 3.2, it is evident that many lakes have a bimodal diurnal variation, with a minor morning peak and a major evening peak in rainfall.

[42] Figure 16a shows that the morning peak is more prominent over larger lakes than over smaller lakes. However, the strength of the diurnal variation in spatially averaged rain rate over the lakes decreases as the size of the lake increases (Figure 16b). When the same number of pixels (two rainfall data grids) were selected for all lakes randomly inside lakes, the strength of the diurnal variation was almost the same for all lakes, and did not correlate with the size of lake (figure not shown). This is because the phase of the diurnal variation is not necessarily uniform over the lake. It is also apparent that the peak in rainfall shifts across the lakes throughout the day. An example is shown in Figure 17, which is a cross section over lake 15 (BB′ in Figure 1). During 1200–1500 LT the rainfall decreases over the center of the lake. During 1500–1800 LT the rain peak shifts from north to south and converges during 1800–2100 LT. It should be noted that rainfall shifts to the center of the lake from the western part of the lake also. During 2100–2400 LT, the rain peak shifts to the steep mountainside. During 0000–0300 LT the rain peak diminishes. During 0600–0900 LT again the rain peak appears over the lake and reduces during 0900–1200 LT. Peak shifts over the lake are clear during 1500–1800 LT to 2100–2400 LT.

[43] Spatial shifting of the rainfall area and the prominent secondary peak during the morning over large lakes might cause a weak average strength of their diurnal variation. Furthermore, in the examination of rainfall peaks over different size lakes, major peaks were observed depending on the basin area of the lake. Figure 18 shows 3-hourly rainfall peak time (e.g., 1200–1400 LT denoted as 1300 LT) versus area of the lake. Figure 18 suggests that the peak rain rate time is delayed as the size of the lake increases. It can

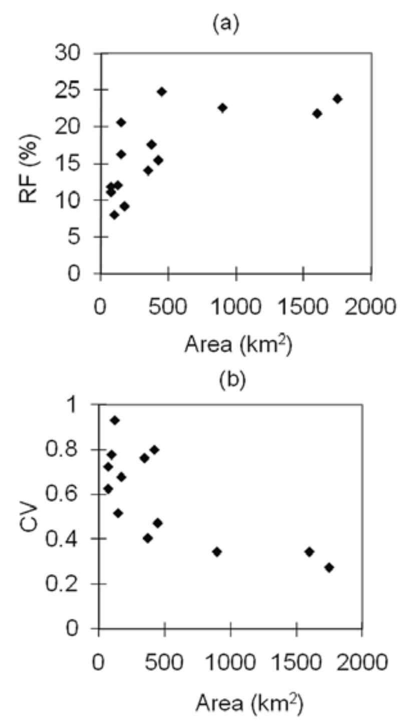

Figure 16. Scatter diagram for lakes of various areas (km^2) (a) versus morning (0300–0900 LT) rain fraction (%) and (b) for strength of diurnal variation (CV).

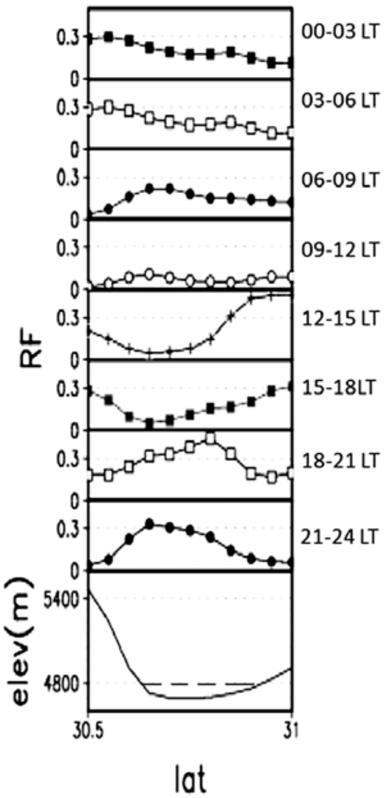

Figure 17. First through eighth panels show rain fraction distribution across Lake 15 (line BB′ in Figure 1). Ninth panel shows basin elevation (meters), and dashed line over the basin shows width of the lake.

be also categorized as lakes with less than 500 km^2 area have rain peaks before 2100 LT and larger lakes have peaks after 2100 LT.

4. Discussion

[44] Because the PR swath is less than 250 km in width, the sample size and statistical significance of rain events over semiarid regions may be poor. However, a comparison of results for the first 5 years (1998–2002) and last 5 years (2003–2007) confirmed the consistency of basic findings. Therefore, by using 10 years of JJA data, the result should be reliable. Including other data, such as TRMM microwave radiometer data, which has a swath 3 times wider, may help to overcome the sampling issues. Another possibility would be to use global rain maps generated from multisatellite data, such as TRMM 3B42 [*Huffman et al.*, 2007] or GSMaP [*Kubota et al.*, 2007]. However, as these data rely on rain estimates derived from microwave radiometer measurements, their accuracy is poor over land. Storm-height data are another unique set of data derived from the PR.

[45] Over the Tibetan Plateau some of the precipitation may be ice or contaminated by the radar bright band over the Tibetan Plateau. However, our result of the spatial distribution of precipitation corresponds to the annual isohyetal map observed by *Yin et al.* [2008] using 94 weather stations over the Plateau. TRMM passes over our study area about 1 time per day at 31°N to 2 times per day at 35°N, on average. So the number of samples over the smallest lake (about 3 rain grids) is approximately more than 2500 for 30 months. But the number of rain samples is not so high being only about 150 for 30 months. Even though the diurnal rain rate of the smallest lake is not identical for first 5 years (1998–2002) and second 5 years (2003–2007), the trends show major features.

[46] In summer, the Tibetan Plateau is characterized by weak prevailing winds, a land surface with some local moisture sources, and strong solar radiation. These factors result in a strong diurnal variation in precipitation. The weak prevailing wind leads to weak baroclinicity, small synoptic-scale disturbances, and precipitation systems caused primarily by local forcing, such as solar radiation and topography. Another important factor is that the central Tibetan Plateau is rather dry even in summer, which means that solar radiation strongly controls precipitation systems. Over the southern flank of the Himalayas, the diurnal variation is strong in the premonsoon season and slightly weaker in the summer mature monsoon season [*Bhatt and Nakamura*, 2005]. A similar phenomenon was revealed for the Amazon area in South America [*Petersen et al.*, 2002]. When the atmosphere is very humid, precipitation systems are very easy to initiate. The summer condition over the Tibetan Plateau may be similar to that in the premonsoon season over India, where the diurnal variation is strongest. Figure 6 shows that the diurnal variation is somewhat weak in August. This may be due to a more humid atmosphere in August. The peak local time of conditional rain rate precedes that of frequency of rain in July, but this is not clear in June, August, or September (Figure 6). Strong rain followed by widespread stratiform rain is a characteristic of large squall line systems [*Zipser*, 1977; *Houze*, 1977; *Leary and Houze*, 1979]. In this case, convective rainfall (the peak time of conditional rain rate) precedes that of stratiform rainfall (frequency of rain). Thus, it is reasonable to suppose that strong mesoscale convective systems dominate in July compared with other months. *Zhu and Chen* [2003] also observed a series of mesoscale convective systems occurred daily over the Plateau during 25–28 July 1995.

[47] *Yamada* [2008] suggested that more persistent rainfall with a high mean rain rate occurs during the wet season. Our results suggest that July and August receive a higher amount of rainfall with more persistent rainfall than June and September (Figures 6 and 7). Persistent rainfall

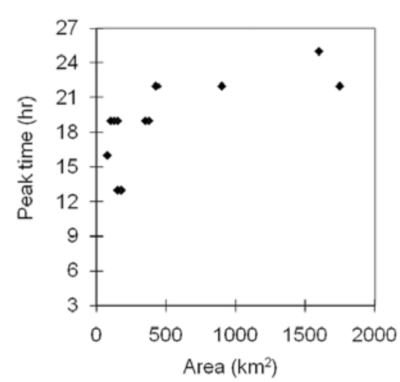

Figure 18. Peak rain rate time (hours) over lakes of various areas (km^2).

appeared during the late-afternoon/evening period in July but during the late-night/morning period in August. It is now known that in some regions morning rain is enhanced in the humid season in relatively low areas [i.e., *Bhatt and Nakamura*, 2005]. This supposition supports the idea that the plateau may be more humid owing to surface moisture in August than in other months. *Yamada and Uyeda* [2006] suggested eastward migration of nocturnal stratiform rain from the western plateau related to the seasonal progress of the moisture during 1998. But we did not investigate rainfall propagation in this study.

[48] Moreover, over the central Tibetan Plateau, the enhancement of persistent morning rain appears most clearly over large lakes. It is very plausible that lakes cause morning rainfall. According to *Stull* [1988], the lake breeze induces divergence (convergence) in the afternoon (morning) over the lake. A deep river valley also shows some persistent morning rain enhancement, but not so distinct. This also suggests that a humid atmosphere is essential for the morning rain peak. Over the Tibetan Plateau, the slope effect may be insufficient to cause a morning rain peak; however, in combination with the large heat capacity of the lake water, it can induce a strong morning rain peak. It is also apparent that the peak rain rate delayed with increasing lake size. It may be that convergence of water vapor is delayed over large lakes.

[49] The effect of diurnal variation on the large-scale circulation is a major issue. Strong diurnal variation in precipitation may mean a vigorous system that causes strong vertical mixing, but this has not been verified. Understanding how local diurnal variations in circulation interact with the large-scale circulation may help to resolve this issue. Several investigations have reported on the spatial propagation of the diurnal variation in convection [e.g., *Carbone et al.*, 2002; *Fujinami et al.*, 2005; *Wang et al.*, 2004, 2005]. This propagation may cause large-scale diurnal variation. *Chow and Chan* [2009] proposed that convergence over the plateau during late afternoon is correlated with divergence over the Bangladesh region. Our study found distinct diurnal variation over hilly regions, valleys, and lakes within the central Tibetan Plateau. The study also revealed the shifting of rain peak location toward and away from land and valley. These are very local phenomena and may not be a direct cause of the diurnal variation in large-scale circulation. However, afternoon to evening precipitation systems generally dominate over the plateau and this may cause a diurnal variation in the large-scale circulation.

5. Summary and Conclusions

[50] This paper explores the diurnal characteristics of rainfall over the central Tibetan Plateau during the monsoon season using the TRMM PR data set for the 10-year period 1998–2007 with a $0.05° \times 0.05°$ grid ($\sim$5 km $\times$ 5 km). Rainfall characteristics are expressed using conditional rain rate, frequency of rain, and storm height.

[51] The Tibetan Plateau has complex terrain above 4000 m. The Himalayan range blocks the Asian summer monsoon circulation and the Plateau receives weak wind and low amounts of precipitation. The rainfall distribution varies by a great amount between the eastern and western part of the Tibetan Plateau. We have studied the central part of the Tibetan Plateau (where rainfall is more uniform), in detail, particularly on a monthly basis.

[52] The summer season (June–August) receives more than 70% of the total annual rainfall and has the highest amplitude of diurnal variation in precipitation. June and September have an afternoon peak in rainfall, whereas July and August have an evening peak in rainfall. July receives the highest amount of rainfall and has the strongest diurnal variation in precipitation. July has distinct characteristics of afternoon convective rainfall followed by persistent rainfall. Results from August indicate more persistent rainfall during the morning than for other months. It may be due to surface moisture during August.

[53] During summer, more than 60% of rainfall on the central Tibetan Plateau occurs in the afternoon, with a peak around late afternoon. However, relatively low land (valleys and lakes) has an evening rainfall peak. Afternoon-dominant regions have broader peaks with stronger diurnal variation than evening-dominant regions. Morning-dominant regions have weak diurnal variation.

[54] Lakes show distinct secondary peaks, which are prominent over large lakes, during the morning. Results also indicated that the peak of rainfall shifts over large lakes, especially during the afternoon. The time of major peaks in rainfall were delayed as the size of lake increased. A shift in rain peak location toward and away from valleys also appeared clearly. However, the relation between surface elevation and diurnal variation is not seen clearly.

[55] The Tibetan Plateau has strong local precipitation systems in summer, and the plateau is a good test region to investigate the effect of local forcing on precipitation systems. Other hilly regions, in southwest Asia, are suitable for comparison with the Tibetan Plateau. Southwest Asia receives a strong monsoon wind, but still shows strong diurnal variations in precipitation. Thus, a similar analysis to that presented in this paper could reveal the effect of small-scale atmospheric conditions.

[56] **Acknowledgments.** The authors would like to thank D. Short, M. L. Shrestha, and H. Fujinami, Nagoya University, for many valuable discussions and for their help in polishing the manuscript. They are grateful to E. J. Zipser and two anonymous reviewers for their comments and suggestions that led to significant improvements in the manuscript. The TRMM data were provided by JAXA. The study was supported by JAXA through the TRMM project.

References

Awaka, J. (1998), Algorithm 2A23-Rain type classification, paper presented at Symposium on the Precipitation Observation from Non-Sun Synchronous Orbit, Earth Sci. Technol. Org., Nagoya, Japan.

Banta, R. M. (1998), The role of mountain flows in making clouds. Chapter 9, *Atmospheric Process over Complex Terrain*, *Meteorol. Monogr.*, vol. 23, edited by W. Blumen, pp. 173–228, Am. Meteorol. Soc., Boston.

Barros, A. P., and T. J. Lang (2003), Monitoring the monsoon in the Himalayas: Observations in central Nepal, June 2001, *Mon. Weather Rev.*, *131*, 1408–1427, doi:10.1175/1520-0493(2003)131<1408:MTMITH>2.0.CO;2.

Barros, A. P., M. Joshi, J. Putkonen, and D. W. Burbank (2000), A study of the 1999 monsoon rainfall in a mountainous region in central Nepal using TRMM products and rain gauge observations, *Geophys. Res. Lett.*, *27*(22), 3683–3686, doi:10.1029/2000GL011827.

Barros, A. P., G. Kim, E. Williams, and S. W. Nesbitt (2004), Probing orographic controls in the Himalayas during the monsoon using satellite imagery, *Nat. Hazards Earth Syst. Sci.*, *4*, 29–51.

Bhatt, B. C., and K. Nakamura (2005), Characteristics of monsoon rainfall around the Himalayas revealed by TRMM precipitation radar, *Mon. Weather Rev.*, *133*, 149–165, doi:10.1175/MWR-2846.1.

Bhatt, B. C., and K. Nakamura (2006), A climatological-dynamical analysis associated with precipitation around the southern part of the Himalayas, *J. Geophys. Res.*, *111*, D02115, doi:10.1029/2005JD006197.

Bhushan, S., and A. P. Barros (2007), A numerical study to investigate the relationship between moisture convergence patterns and orography in central Mexico, *J. Hydrometeorol.*, *8*, 1264–1284, doi:10.1175/2007JHM791.1.

Carbone, R. E., J. D. Tuttle, D. A. Ahijevych, and S. B. Trier (2002), Inferences of predictability associated with warm season precipitation episode, *J. Atmos. Sci.*, *59*(13), 2033–2056, doi:10.1175/1520-0469(2002)059<2033:IOPAWW>2.0.CO;2.

Chow, C. K., and J. C. L. Chan (2009), Diurnal variation of circulation and precipitation in the vicinity of the Tibetan Plateau in early summer, *Clim. Dyn.*, *32*, 55–73, doi:10.1007/s00382-008-0374-x.

Dai, A. (2001), Global precipitation and thunderstorm frequencies. Part II: Diurnal variations, *J. Clim.*, *14*, 1112–1128, doi:10.1175/1520-0442(2001)014<1112:GPATFP>2.0.CO;2.

Dai, A., X. Lin, and K. Hsu (2007), The frequency, intensity, and diurnal cycle of rainfall in surface and satellite observations over low- and mid-latitudes, *Clim. Dyn.*, *29*, 727–744, doi:10.1007/s00382-007-0260-y.

Flohn, H. (1957), Large-scale aspects of the 'summer monsoon' in South and East Asia, *J. Meteorol. Soc. Jpn.*, *35*, 180–186.

Fu, Y., and G. Liu (2007), Possible misidentification of rain type by TRMM PR over Tibetan Plateau, *J. Appl. Meteorol. Climatol.*, *46*, 667–672, doi:10.1175/JAM2484.1.

Fujinami, H., and T. Yasunari (2001), The seasonal and intraseasonal variability of diurnal cloud activity over the Tibetan Plateau, *J. Meteorol. Soc. Jpn.*, *79*, 1207–1227, doi:10.2151/jmsj.79.1207.

Fujinami, H., S. Nomura, and T. Yasunari (2005), Charecteristics of diurnal variations in convection and precipitation over the southern Tibetan Plateau during summer, *SOLA*, *1*, 49–51, doi:10.2151/sola.2005-014.

Hirose, M., and K. Nakamura (2005), Spatial and diurnal variation of precipitation systems over Asia observed by the TRMM precipitation radar, *J. Geophys. Res.*, *110*, D05106, doi:10.1029/2004JD004815.

Hirose, M., R. Oki, S. Shimizu, M. Kachi, and T. Higashiuwatoko (2008), Fine scale diurnal rainfall statistics refined from eight years of TRMM PR data, *J. Appl. Meteorol. Climatol.*, *47*, 544–561, doi:10.1175/2007JAMC1559.1.

Houze, R. A., Jr. (1977), Structure and dynamics of a tropical squall-line system, *Mon. Weather Rev.*, *105*, 964–980, doi:10.1175/1520-0493(1977)105<0964:RCOTCO>2.0.CO;2.

Huffman, G. L., R. F. Adler, D. T. Bolvin, G. Gu, E. J. Nelkin, K. P. Bowman, Y. Hong, E. F. Stocker, and D. B. Wolff (2007), The TRMM multi-satellite precipitation analysis: Quasi-global, multi-year, combined-sensor precipitation estimates at fine scale, *J. Hydrometeorol.*, *8*, 38–55, doi:10.1175/JHM560.1.

Iguchi, T., T. Kozu, R. Meneghini, J. Awaka, and K. Okamoto (2000), Rain-profiling algorithm for the TRMM precipitation radar, *J. Appl. Meteorol.*, *39*, 2038–2052, doi:10.1175/1520-0450(2001)040<2038:RPAFTT>2.0.CO;2.

Kondo, Y., A. Higuchi, and K. Nakamura (2006), Small-scale cloud activity over the maritime continent and the western Pacific as revealed by satellite data, *Mon. Weather Rev.*, *134*, 1581–1599, doi:10.1175/MWR3132.1.

Krishnamurti, T. N., and C. M. Kishtawal (2000), A pronounced continental-scale diurnal mode of the Asian summer monsoon, *Mon. Weather Rev.*, *128*, 462–473, doi:10.1175/1520-0493(2000)128<0462:APCSDM>2.0.CO;2.

Kubota, H., and T. Nitta (2001), Diurnal variation of tropical convection observed during the TOGA-COARE, *J. Meteorol. Soc. Jpn.*, *79*, 815–830, doi:10.2151/jmsj.79.815.

Kubota, T., et al. (2007), Global precipitation map using satellite-borne microwave radiometers by the GSMaP Project: Prodution and validataion, *IEEE Trans. Geosci. Remote Sens.*, *45*, 2259–2275, doi:10.1109/TGRS.2007.895337.

Kuwagata, T., A. Numaguti, and N. Endo (2001), Diurnal variation of water vapor over the central Tibetan Plateau during summer, *J. Meteorol. Soc. Jpn.*, *79*, 401–418, doi:10.2151/jmsj.79.401.

Lang, T. J., and A. P. Barros (2002), An investigation of the onsets of the 1999 and 2000 monsoons in central Nepal, *Mon. Weather Rev.*, *130*, 1299–1316, doi:10.1175/1520-0493(2002)130<1299:AIOTOO>2.0.CO;2.

Leary, C. A., and R. A. Houze (1979), The structure and evolution of convection in a tropical cloud cluster, *J. Atmos. Sci.*, *36*, 437–457, doi:10.1175/1520-0469(1979)036<0437:TSAEOC>2.0.CO;2.

Li, C., and M. Yanai (1996), The onset and interannual variability of the Asian summer monsoon in relation to land-sea thermal contrast, *J. Clim.*, *9*, 358–375, doi:10.1175/1520-0442(1996)009<0358:TOAIVO>2.0.CO;2.

Lin, X., D. A. Randall, and L. D. Fowler (2000), Diurnal variability of the hydrologic cycle and radiative fluxes: Comparisons between observations and a GCM, *J. Clim.*, *13*, 4159–4179, doi:10.1175/1520-0442(2000)013<4159:DVOTHC>2.0.CO;2.

Luo, H., and M. Yanai (1983), The large-scale circulation and heat sources over the Tibetan Plateau and surrounding areas during the early summer of 1979. Part I: Precipitation and kinematic analysis, *Mon. Weather Rev.*, *111*, 922–944, doi:10.1175/1520-0493(1983)111<0922:TLSCAH>2.0.CO;2.

Murakami, T. (1987), Orography and monsoons, in *Monsoons*, edited by J. S. Fein and P. L. Stephens, pp. 331–364, John Wiley, Hoboken, N. J.

Negri, A. J., R. F. Adler, E. J. Nelkin, and G. J. Huffman (1994), Regional rainfall climatologies derived from Special Sensor Microwave Imager (SSM/I) data, *Bull. Am. Meteorol. Soc.*, *75*, 1165–1182, doi:10.1175/1520-0477(1994)075<1165:RRCDFS>2.0.CO;2.

Nesbitt, S. W., and E. J. Zipser (2003), The diurnal cycle of rainfall and convective intensity according to three years of TRMM measurements, *J. Clim.*, *16*, 1456–1475.

Nitta, T. (1983), Observational study of heat sources over the eastern Tibetan Plateau during the summer monsoon, *J. Meteorol. Soc. Jpn.*, *61*, 590–605.

Nitta, T., and S. Sekine (1994), Diurnal variation of convective activity over the tropical western Pacific, *J. Meteorol. Soc. Jpn.*, *72*, 627–640.

Ohsawa, T., H. Ueda, T. Hayashi, A. Watanabe, and J. Matsumoto (2001), Diurnal variations of convective activity and rainfall in tropical Asia, *J. Meteorol. Soc. Jpn.*, *79*, 333–352, doi:10.2151/jmsj.79.333.

Petersen, W. A., S. W. Nesbitt, R. J. Blakeslee, R. Cifelli, P. Hein, and S. A. Rutledge (2002), TRMM observations of intraseasonal variability in convective regimes over the Amazon, *J. Clim.*, *15*, 1278–1294, doi:10.1175/1520-0442(2002)015<1278:TOOIVI>2.0.CO;2.

Reihl, H. (1954), *Tropical Meteorology*, 392 pp., McGraw-Hill, New York.

Sato, T., F. Kimura, and A. S. Hasegawa (2007), Vegetation and topographic control of cloud activity over arid/semiarid Asia, *J. Geophys. Res.*, *112*, D24109, doi:10.1029/2006JD008129.

Schumacher, C., and R. A. Houze (2003), Stratiform rain in the tropics as seen by the TRMM precipitation radar, *J. Clim.*, *16*, 1739–1756.

Shimizu, S., K. Ueno, H. Fujii, H. Yamada, R. Shiroka, and L. P. Liu (2001), Mesoscale characteristics and structures of stratiform rainfall on the Tibetan Plateau, *J. Meteorol. Soc. Jpn.*, *79*, 435–461, doi:10.2151/jmsj.79.435.

Singh, P., F. A. Furuzawa, and K. Nakamura (2005), Diurnal variation of rainfall over Himalayan region, in *Landschaftsökologie und Umweltforschung*, vol. 48, edited by A. Herrmann, pp. 5–10, Tech. Univ. Braunschweig, Braunschweig, Germany.

Stull, R. B. (1988), *An Introduction to Boundary Layer Meteorology*, 666 pp., Kluwer Acad., Norwell, Mass.

Tian, B., I. M. Held, N. C. Lau, and B. J. Soden (2005), Diurnal cycle of summertime deep convection over North America: A satellite perspective, *J. Geophys. Res.*, *110*, D08108, doi:10.1029/2004JD005275.

Ueno, K., H. Fujii, H. Yamada, and L. P. Liu (2001), Weak and frequent monsoon rainfall over the Tibetan Plateau, *J. Meteorol. Soc. Jpn.*, *79*, 419–434, doi:10.2151/jmsj.79.419.

Ueno, K., K. Tanaka, H. Tsutsui, and M. S. Li (2007), Snow cover conditions in the Tibetan Plateau observed during the winter of 2003/2004, *Arct. Antarct. Alp. Res.*, *39*, 152–164, doi:10.1657/1523-0430(2007)39[152:SCCITT]2.0.CO;2.

Uyeda, H., H. Yamada, J. Horikomi, R. Shirooka, S. Shimizu, L. P. Liu, K. Ueno, H. Fujii, and T. Koike (2001), Characteristics of convective clouds observed by a Doppler radar at Naqu on Tibetan Plateau during the GAME-Tibet IOP, *J. Meteorol. Soc. Jpn.*, *79*, 463–474, doi:10.2151/jmsj.79.463.

Wang, C.-C., G. T. J. Chen, and R. E. Carbone (2004), A climatology of warm-season cloud patterns over east Asia based on GMS infrared brightness temperature observations, *Mon. Weather Rev.*, *132*, 1606–1629, doi:10.1175/1520-0493(2004)132<1606:ACOWCP>2.0.CO;2.

Wang, C.-C., G. T. J. Chen, and R. E. Carbone (2005), Variability of warm-season cloud episodes over east Asia based on GMS infrared brightness temperature observations, *Mon. Weather Rev.*, *133*, 1478–1500, doi:10.1175/MWR2928.1.

Yamada, H. (2008), Numerical simulations of the role of land surface conditions in the evolution and structure of summertime thunderstorms over a flat highland, *Mon. Weather Rev.*, *136*, 173–188, doi:10.1175/2007MWR2053.1.

Yamada, H., and H. Uyeda (2006), Transition of the rainfall characteristics related to the moistening of the land surface over the central Tibetan Plateau during the summer of 1998, *Mon. Weather Rev.*, *134*, 3230–3247, doi:10.1175/MWR3235.1.

Yamamoto, K. M., F. A. Furuzawa, A. Higuchi, and K. Nakamura (2008), Comparison of diurnal variations in precipitation systems observed by TRMM PR, TMI, and VIRS, *J. Clim.*, *21*, 4011–4028, doi:10.1175/2007JCLI2079.1.

Yanai, M., and C. F. Li (1994), Mechanism of heating and the boundary layer over the Tibetan Plateau, *Mon. Weather Rev.*, *122*, 305–323, doi:10.1175/1520-0493(1994)122<0305:MOHATB>2.0.CO;2.

Yanai, M., C. Li, and Z. Song (1992), Seasonal heating of the Tibetan Plateau and its effects on the evolution of Asian summer monsoon, *J. Meteorol. Soc. Jpn.*, *70*, 319–351.

Yin, Z., X. Zhang, X. Liu, M. Colella, and X. Chen (2008), An assessment of the biases of satellite rainfall estimates over the Tibetan Plateau and correction methods based on topographic analysis, *J. Hydrometeorol.*, *9*, 301–326, doi:10.1175/2007JHM903.1.

Yu, R., T. Zhou, A. Xiong, Y. Zhu, and J. Li (2007), Diurnal variations of summer rainfall over contiguous China, *Geophys. Res. Lett.*, *34*, L01704, doi:10.1029/2006GL028129.

Zhu, G., and S. Chen (2003), Analysis and comparison of mesoscale convective systems over the Qinghai-Xizang (Tibetan) Plateau, *Adv. Atmos. Sci.*, *20*, 311–322, doi:10.1007/BF02690789.

Zipser, E. J. (1977), Mesoscale and convective-scale downdrafts as distinct components of squall line structure, *Mon. Weather Rev.*, *105*, 1568–1589, doi:10.1175/1520-0493(1977)105<1568:MACDAD>2.0.CO;2.

K. Nakamura, Hydrospheric Atmospheric Research Center, Nagoya University, Furocho, Chikusa-ku, Nagoya 464-8601, Japan.

P. Singh, Graduate School of Environmental Studies, Furocho, Chikusa-ku, Nagoya 464-8601, Japan. (prasamsasingh@gmail.com)